International Journal of Science and Research (IJSR)
ISSN: 2319-7064
Impact Factor 2025: 7.089

Juvenile Metachromatic Leukodystrophy Masquerading as Communicating Hydrocephalus: A Diagnostic Challenge

Dr. Naragoni Ankitha Swarna Bharathi[1], Dr. Darsh Anoop Sandhu[2], Dr. Ganesh Avhad[3]

[1]Department of Radiodiagnosis, Dr. D.Y Patil Medical College, Nerul, Navi Mumbai, India
Email: *Ankitha06111998[at]gmail.com*

[2]Department of Radiodiagnosis, Dr. D.Y Patil Medical College, Nerul, Navi Mumbai, India
Email: *darshsandhu.99[at]gmail.com*

[3]Department of Radiodiagnosis, Dr. D.Y Patil Medical College, Nerul, Navi Mumbai, India
Email: *drganesh_gmc[at]hotmail.com*

Abstract: ***Background*: Juvenile metachromatic leukodystrophy (MLD) is a rare autosomal recessive lysosomal storage disorder caused by deficiency of arylsulfatase A, leading to progressive sulfatide accumulation and central nervous system demyelination. Its insidious onset and nonspecific early clinical features render it susceptible to diagnostic delay, particularly when co-existing structural brain abnormalities provide an apparently adequate explanation for neurological deterioration. *Case Presentation*: We report a child with a background of communicating hydrocephalus and a ventriculoperitoneal (VP) shunt who presented with fever, altered behaviour, and regression of previously acquired developmental milestones. The referring team considered subacute sclerosing panencephalitis and chronic meningitis as primary differential diagnoses. MRI of the brain with plain and contrast sequences demonstrated mild ventriculomegaly (Evans index 0.38), significant corpus callosum thinning, and bilateral T2/FLAIR hyperintensities involving the periventricular and deep white matter of the bilateral fronto-temporo-parietal regions with corresponding T1 hypointensity. Post-contrast imaging revealed patchy enhancement within the white matter lesions, indicating active demyelination. Diffusion-weighted imaging showed facilitated diffusion consistent with chronic demyelination. MR spectroscopy of the abnormal white matter demonstrated lipid peaks at 0.9 and 1.3 ppm, elevated choline at 3.2 ppm, and markedly reduced N-acetylaspartate at 2.0 ppm- a metabolic profile characteristic of an active leukodystrophic process. Juvenile MLD was proposed as the leading radiological differential diagnosis, with biochemical confirmation by arylsulfatase A enzyme assay recommended.***

Keywords: Leukodystrophy, Metachromatic; Hydrocephalus, Communicating; Magnetic Resonance Spectroscopy; White Matter-pathology; Arylsulfatase A- deficiency

1. Introduction

Metachromatic leukodystrophy (MLD) is a rare autosomal recessive lysosomal storage disorder caused by deficient activity of the enzyme arylsulfatase A (ARSA), encoded by the *ARSA* gene on chromosome 22q13.3. This enzymatic deficiency results in the pathological accumulation of sulfatides within the myelin sheaths of both the central and peripheral nervous systems, leading to progressive demyelination and neurological deterioration [1]. The disease was first described in its molecular basis by Polten et al., who demonstrated that specific *ARSA* allelic mutations determine the clinical form of the disease [2]. The birth prevalence of MLD varies across populations but has been estimated to be between 1 in 40,000 and 1 in 160,000. Three clinical subtypes are recognised based on age at symptom onset: late-infantile (onset ≤ 2.5 years), juvenile (onset 2.5 to < 16 years), and adult (onset ≥ 16 years) [3].

The juvenile form of MLD, which is the subject of this report, typically manifests between the ages of 2.5 and 16 years and is characterised by a more protracted and variable disease course compared to the late-infantile subtype [4]. Clinical presentation commonly includes regression of previously acquired milestones, progressive cognitive decline, behavioural changes, and motor dysfunction, with peripheral neuropathy often preceding overt central nervous system manifestations [1]. This insidious and nonspecific symptom onset frequently leads to diagnostic delay. In children diagnosed at six years of age or younger, general neurologic concerns, gastrointestinal symptoms, seizures, and language-related events were among the most common pre-diagnostic presentations, with a median time to MLD diagnosis exceeding 230 days from the onset of the first prodromal cluster.

Neuroimaging, particularly magnetic resonance imaging (MRI) of the brain, plays a pivotal role in the recognition and characterisation of MLD. MRI has become the primary imaging modality in patients with leukodystrophy, playing an important role in the identification, localisation, and characterisation of underlying white matter abnormalities. The characteristic MRI pattern in MLD comprises bilateral confluent T2/FLAIR hyperintensities involving the periventricular and deep white matter, with a predilection for the fronto-parietal regions, typically sparing the subcortical U-fibres in the early stages. The "tigroid" or "leopard skin" pattern- reflecting islands of preserved myelin within the demyelinated white matter- is considered pathognomonic [5]. Involvement of the corpus callosum has been identified as a characteristic early MRI sign, present in 94% of symptomatic early-juvenile and 100% of symptomatic late-juvenile and adult MLD patients. A standardised MRI scoring system has been developed for MLD, enabling quantification of white

matter disease burden along a 34-point scale based on lesion location and global atrophy, which has proven valuable for longitudinal disease monitoring and treatment evaluation [6]. In juvenile MLD, high MRI severity scores are often evident already at disease onset and even in presymptomatic patients, and the temporal patterns of MRI progression are more variable than in the late-infantile form. MR spectroscopy (MRS) provides complementary metabolic information to conventional MRI and has an established role in characterising the neurochemical milieu of MLD-affected white matter. The most pronounced MRS differences in MLD compared to controls are found in the white matter, with larger values corresponding to the main peaks of myo-inositol, choline, and aspartate, and smaller values associated with NAA and glutamine. Reduced N-acetylaspartate (NAA) reflects neuronal and axonal loss, while elevated choline indicates active membrane turnover from ongoing demyelination, and the presence of lipid peaks signifies myelin breakdown products [7].

The diagnostic challenge posed by MLD is compounded when the imaging findings are atypical or when a coexisting structural abnormality, such as hydrocephalus, dominates the clinical picture. Communicating hydrocephalus, characterised by ventriculomegaly with an Evans index exceeding 0.3, may arise from a variety of aetiologies in the paediatric population and can independently cause milestone regression, thus potentially diverting clinical attention away from an underlying leukodystrophic process [8]. The co-occurrence of a ventriculoperitoneal (VP) shunt — placed for hydrocephalus — alongside an undiagnosed leukodystrophy represents a particularly treacherous diagnostic scenario, as neurological deterioration may be incorrectly attributed to shunt malfunction or disease progression of the hydrocephalus alone. In early or presymptomatic disease stages, the typical MRI changes of MLD might be absent, hampering early diagnosis, and knowledge of these early MRI signs is important for fast diagnosis.

We herein report a case of juvenile MLD presenting with communicating hydrocephalus and a pre-existing VP shunt, in which the underlying leukodystrophic diagnosis was established by MRI brain with contrast, incorporating diffusion-weighted imaging and MR spectroscopy. This case highlights the critical importance of systematic multiparametric MRI evaluation and the role of MRS as a discriminating diagnostic tool in children with neurological regression, even in the setting of a known structural brain abnormality [9,10].

2. Case Presentation

A child aged 8 years brought by his mother, presented with a history of hemiparesis on the right side dating back to 2023. The patient had a previously documented diagnosis of communicating hydrocephalus with periventricular white matter hyperintensities extending to the left-sided gangliocapsular and thalamic regions, for which a ventriculoperitoneal (VP) shunt was surgically placed in June 2025. The current presentation was precipitated by a complaint of fever persisting for one month, documented at 100–101°F with two spikes per day, which remained active during the interfebrile period. In addition to the fever, the caregivers reported altered behaviour and regression of previously acquired developmental milestones. On systemic evaluation, the patient was referred to the ENT department, where anterior rhinoscopy revealed a polypoid mass in the left nasal cavity, and throat examination demonstrated bilateral grade 1 tonsillar enlargement. The referring clinical team entertained a differential diagnosis of subacute sclerosing panencephalitis (SSPE) and chronic meningitis given the clinical constellation of milestone regression, fever, and altered behaviour.

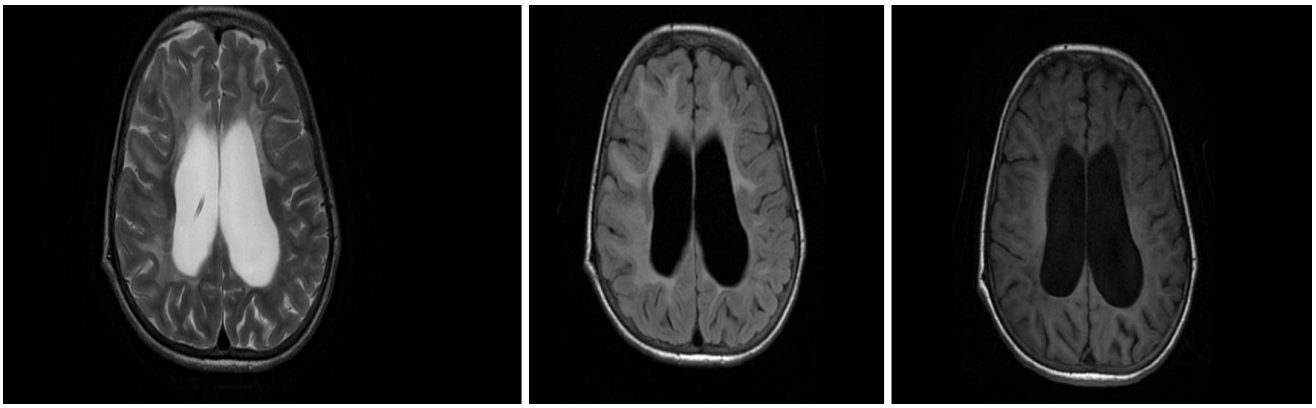

Figure 1: Axial MRI sequences. Left: T2-weighted image showing markedly enlarged lateral ventricles with bilateral periventricular white matter T2 hyperintensities. Middle: FLAIR image demonstrating dilated ventricles and confluent periventricular signal abnormality. Right: T1-weighted image showing bilateral T1 hypointensity in the periventricular and deep white matter corresponding to demyelination.

In view of the neurological deterioration, an MRI of the brain with plain and contrast sequences was performed. On the MRI, a burr hole defect was identified in the right parietal region, consistent with the prior surgical history. The VP shunt tube was visualised traversing through the right parietal lobe with its tip appropriately positioned in the right frontal lobe. Mild ventriculomegaly was noted involving the lateral, third, and fourth ventricles, with an Evans index of 0.38, the findings being most consistent with communicating hydrocephalus. Significant thinning of the corpus callosum was identified, a finding well-recognised in advanced white matter disease. T2-weighted and FLAIR sequences

demonstrated bilateral hyperintensities involving the periventricular white matter in the bilateral fronto-temporo-parietal regions, as well as the subcortical and deep white matter of the bilateral frontal lobes; corresponding T1-weighted hypointensity was noted in the same distribution.

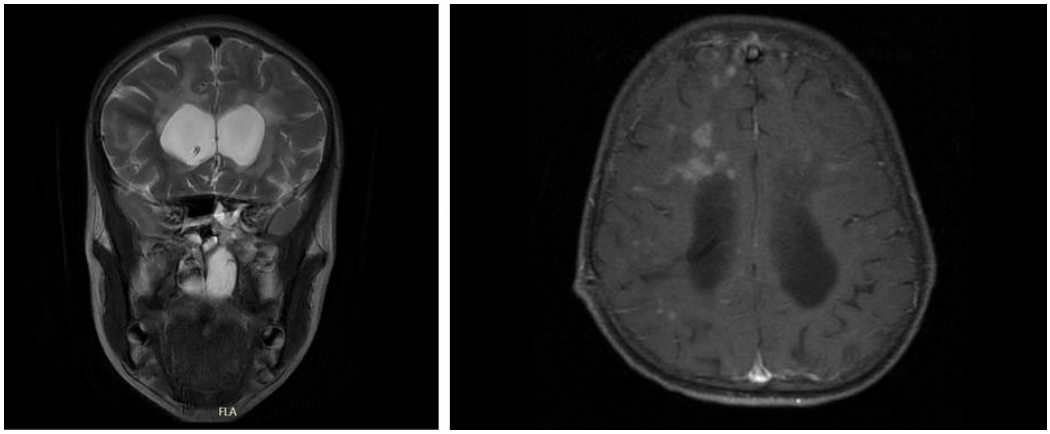

Figure 2: Left: Coronal T2-weighted image demonstrating bilateral symmetric ventriculomegaly and extensive periventricular white matter hyperintensity. Right: Axial post-contrast T1-weighted image showing patchy enhancement within the periventricular white matter lesions, indicating active demyelination.

On post-contrast administration, the white matter lesions demonstrated patchy enhancement, indicating active demyelination. Diffusion-weighted imaging showed no evidence of restricted diffusion within the white matter lesions, with the apparent diffusion coefficient (ADC) map confirming facilitated diffusion, a pattern consistent with chronic demyelination rather than acute infarction.

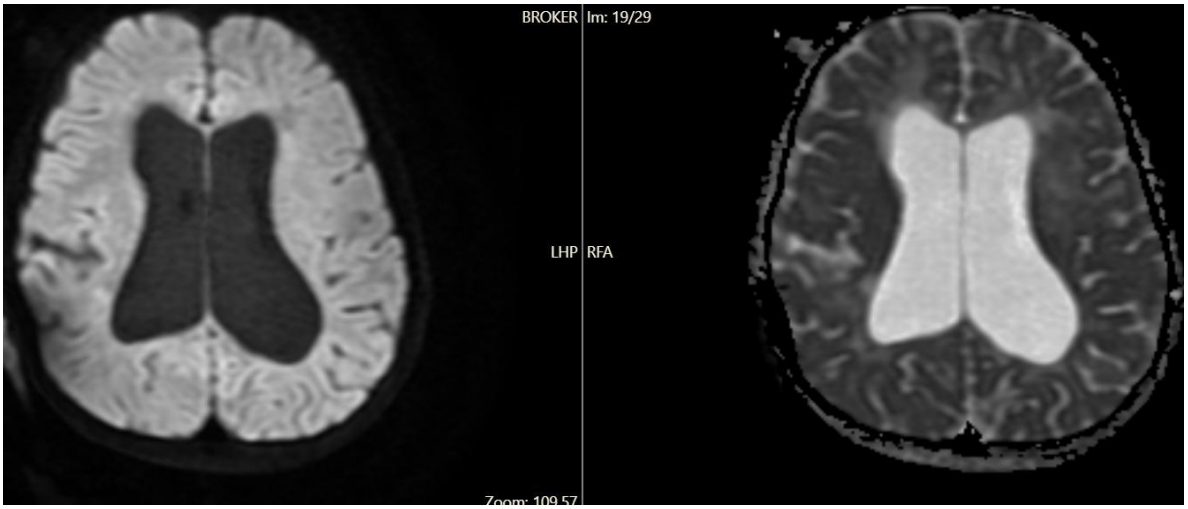

Figure 3: Diffusion-weighted imaging (DWI, left) and apparent diffusion coefficient (ADC) map (right). The periventricular white matter lesions show no restricted diffusion on DWI, with corresponding facilitated diffusion (bright signal) on the ADC map, consistent with chronic demyelination rather than acute ischaemia.

MR spectroscopy was performed as a targeted adjunct to characterise the metabolic profile of the abnormal white matter. The spectroscopic trace demonstrated a lipid peak at 0.9 ppm and 1.3 ppm, consistent with myelin breakdown products. An elevated choline peak was identified at 3.2 ppm, reflecting active membrane turnover and ongoing demyelination. Markedly reduced N-acetylaspartate (NAA) peak was recorded at 2.0 ppm, indicating significant neuronal and axonal loss within the affected white matter.

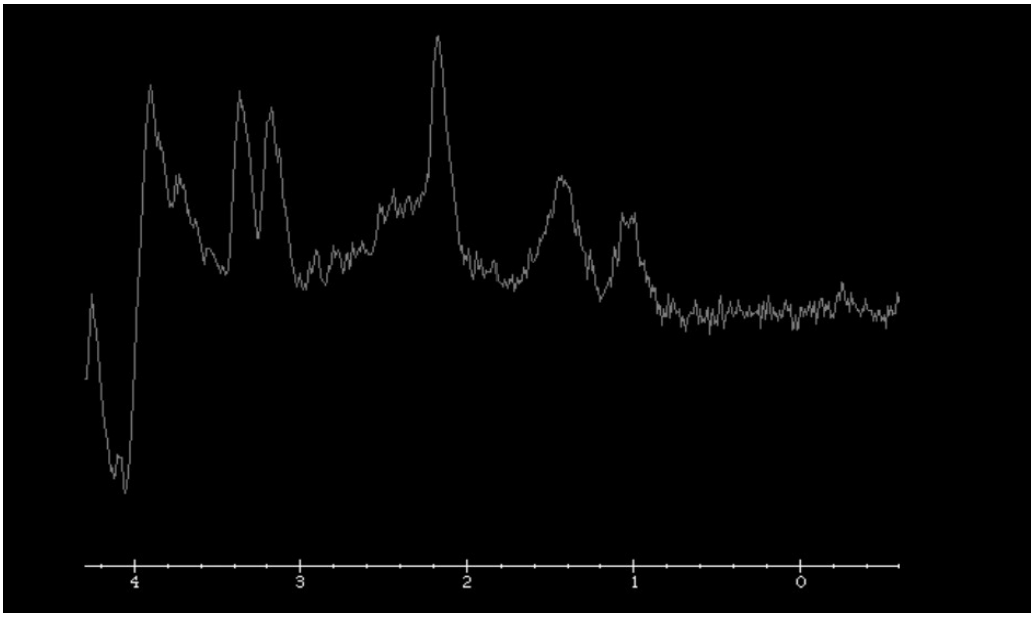

Figure 4: MR Spectroscopy trace from the periventricular white matter. Note the prominent lipid peaks at 0.9 and 1.3 ppm (myelin breakdown products), elevated choline peak at 3.2 ppm (active demyelination), and markedly reduced NAA peak at 2.0 ppm (neuronal/axonal loss). This spectroscopic pattern is characteristic of an active leukodystrophic process.

This specific spectroscopic pattern- combining lipid peaks, elevated choline, and profoundly depressed NAA- in the context of the bilateral periventricular and deep white matter T2/FLAIR hyperintensities with corpus callosum thinning and the clinical background of milestone regression, led the radiologist to propose the following possible radiological differentials: (1) juvenile metachromatic leukodystrophy, (2) other leukodystrophy, and (3) inflammatory or infectious leukoencephalopathy. Juvenile metachromatic leukodystrophy was listed as the leading differential diagnosis, and biochemical confirmation by measurement of arylsulfatase A enzyme activity in leukocytes and urine sulfatide estimation was recommended for definitive diagnosis.

3. Discussion

The present case illustrates the diagnostic complexity that arises when juvenile metachromatic leukodystrophy (MLD) co-exists with, and is overshadowed by, a known structural brain abnormality- in this instance, communicating hydrocephalus managed with a ventriculoperitoneal (VP) shunt. Our patient, a child with a background of right-sided hemiparesis and prior shunt surgery, presented with fever, behavioural change, and regression of developmental milestones. The clinical team appropriately considered SSPE and chronic meningitis as primary differentials. However, multiparametric MRI, particularly MR spectroscopy, ultimately raised juvenile MLD as the leading radiological diagnosis. This sequence of events underscores a well-recognised but underemphasised challenge in paediatric neurology: when a pre-existing diagnosis is present, the threshold for considering an additional or superseding pathology is often raised, leading to diagnostic delay [9]. Mohajer et al. (2025), in a large real-world data analysis of 174 MLD cases diagnosed at or below age six, found that neurological concerns preceded MLD diagnosis by a median of 257 days, with language, behavioural, and motor events all documented in the prodromal window - a pattern closely mirroring the presentation in our case [9].

The co-occurrence of communicating hydrocephalus with MLD, as seen in our patient, is a recognised but uncommonly reported association. Desai and Grimm (2013) described a case of MLD presenting with communicating hydrocephalus, concluding that ventriculomegaly in MLD may arise from a combination of periventricular white matter volume loss, reduced overall white matter bulk, and impaired CSF absorption secondary to demyelination-associated inflammatory changes at the arachnoid granulations [11]. In our patient, the Evans index of 0.38 confirmed ventriculomegaly; yet the bilateral periventricular T2/FLAIR white matter signal abnormality, the significant corpus callosum thinning, and the patchy post-contrast enhancement collectively argued against hydrocephalus as the sole explanation for the neurological decline. The existence of a VP shunt added further interpretive complexity: neurological deterioration could easily have been attributed to shunt malfunction rather than an evolving leukodystrophic process, highlighting how prior structural interventions may inadvertently obscure an underlying metabolic disease.

The MRI white matter findings in our case are consistent with the established literature on juvenile MLD. Eichler et al. (2009), in their landmark study developing a 34-point MRI severity scoring system for MLD across 28 patients, described the characteristic pattern as bilateral T2 hyperintensity enveloping the frontal and parietal periventricular and central white matter - faint in mild disease but becoming confluent and denser with progression [6]. They noted that corpus callosum involvement occurs in mild disease and that the tigroid pattern- radially oriented bands of preserved signal intensity within the demyelinated white matter- is characteristic of severe disease across all MLD subtypes, including the juvenile form [6]. Kim et al. (1997), in an MRI study of seven children with childhood MLD, reported symmetric confluent T2 hyperintensity in the

periventricular white matter and centrum semiovale in all cases, with involvement of the genu and splenium of the corpus callosum in five and six patients respectively, and a consistent posterior predominance of the signal abnormality [12]. The fronto-temporo-parietal distribution, periventricular and deep white matter involvement, and significant callosal thinning in our case mirror these established descriptions closely. Schoenmakers et al. (2022), in a retrospective review of 104 MLD brain MRIs across two European centres, further confirmed that corpus callosum demyelination is a sensitive early MRI sign of juvenile MLD, present in 94% of symptomatic early-juvenile patients and in 100% of symptomatic late-juvenile cases, and therefore a key imaging anchor for narrowing the differential diagnosis [7].

A notable and somewhat atypical feature in our case was the presence of patchy post-contrast enhancement within the periventricular white matter lesions, indicative of active blood-brain barrier disruption. In the classical description of MLD, demyelinated white matter typically does not enhance on post-contrast T1-weighted images- a feature historically used to distinguish MLD from active inflammatory demyelinating conditions. Kim et al. (1997) explicitly documented the absence of lesion enhancement on five post-contrast examinations in their childhood MLD cohort [12]. However, enhancement has been described in a subset of MLD patients during phases of heightened inflammatory activity, and Cheon et al. (2002) noted that punctate foci of contrast enhancement may appear within the tigroid pattern, representing perivascular zones of active demyelination [5]. The presence of enhancement in our patient therefore does not exclude MLD; rather, it indicates an active phase of demyelination temporally coinciding with the clinical deterioration, and serves as an important reminder that the absence of enhancement should not be treated as a mandatory criterion for the diagnosis.

The diffusion-weighted imaging (DWI) in our case showed no restricted diffusion within the white matter lesions, with facilitated diffusion confirmed on the ADC map- consistent with established or chronic demyelination rather than acute ischaemia or cytotoxic oedema. This finding is well-supported in the literature. Sener (2002) reported that demyelinated white matter in MLD characteristically demonstrates elevated ADC values reflecting increased water mobility due to myelin and axonal loss, with restricted diffusion encountered only exceptionally in acute disease phases or at specific anatomical sites [13]. The DWI findings in our patient thus served a critical discriminatory function, effectively excluding acute cerebral infarction and acute encephalitis as causes of the clinical deterioration, and directing attention towards a chronic progressive demyelinating aetiology.

The MR spectroscopy findings in our case were pivotal in raising juvenile MLD as the primary differential. The spectroscopic trace demonstrated lipid peaks at 0.9 and 1.3 ppm, an elevated choline peak at 3.2 ppm, and markedly reduced NAA at 2.0 ppm. This metabolic profile is well-characterised in the MLD literature. Feldmann et al. (2023), in a systematic MRS study of 29 MLD patients (including 19 juvenile cases) using a semi-LASER CSI sequence, demonstrated that MLD spectra differed significantly from controls, with the most pronounced white matter changes comprising elevated myo-inositol, elevated choline, and markedly reduced NAA and glutamine [4]. They established that the NAA peak correlated most strongly with motor function ($r = -0.75$; $p < 0.001$) and cognitive function by IQ ($r = 0.84$; $p < 0.001$), confirming NAA as the most clinically meaningful MRS biomarker for disease severity in MLD [4]. The elevated choline in our patient reflects active membrane disruption from ongoing demyelination, while the markedly reduced NAA signals substantial neuronal and axonal loss indicative of advanced disease. The lipid peaks at 0.9 and 1.3 ppm are consistent with free fatty acid release from myelin catabolism. Neyaz et al. (2015), in a prospective MRS study of 26 children with leukodystrophies, confirmed that elevated Cho/Cr, elevated Cho/NAA, and reduced NAA/Cr ratios were the dominant spectroscopic findings across the leukodystrophies studied, and that MRS provides valuable complementary information to conventional MRI in establishing the diagnosis [14].

The clinical differentials initially entertained- SSPE and chronic meningitis- warrant specific discussion in the context of the radiological findings. SSPE characteristically produces cortical and subcortical signal changes with posterior predominance, basal ganglia involvement, and may show gyral enhancement; DWI typically shows cortical restricted diffusion, which was absent in our patient. Chronic meningitis, while capable of producing leptomeningeal enhancement and hydrocephalus, does not explain bilateral confluent periventricular white matter signal abnormality with corpus callosum thinning and the specific spectroscopic profile seen in our case. Furthermore, a recent case report by Lewis et al. (2025) highlighted that MLD may present atypically- with cranial nerve enhancement mimicking an acquired inflammatory demyelinating condition — before classic white matter changes develop, further reinforcing the indispensable role of MRS and multiparametric MRI in establishing the correct diagnosis in atypical or complex presentations [15].

The diagnostic conclusion has pressing therapeutic implications. Groeschel et al. (2016), in a landmark case-control study comparing 26 transplanted with 35 non-transplanted juvenile MLD patients, demonstrated that allogeneic hematopoietic stem cell transplantation (HSCT) significantly slowed cognitive decline in patients with preserved neurological function at the time of transplantation, with the best outcomes observed in patients with minimal motor deficit (GMFC-MLD grade 0) and low MRI severity scores (≤17) [16]. More recently, Fumagalli et al. (2022) reported long-term results from the phase 1/2 trial of atidarsagene autotemcel (arsa-cel, Libmeldy/Lenmeldy) in 29 patients with early-onset MLD, demonstrating that presymptomatic and early-symptomatic patients treated with this lentiviral haematopoietic stem cell gene therapy had substantially better neurodevelopmental outcomes compared to the natural history cohort, over a maximum follow-up of 7.5 years [17]. Atidarsagene autotemcel received FDA approval in March 2024 for presymptomatic late-infantile, presymptomatic early-juvenile, and early-symptomatic early-juvenile MLD, representing a paradigm shift in the management of this condition [17]. For our patient, prompt biochemical confirmation- arylsulfatase A enzyme activity in

leukocytes and ARSA gene sequencing- is therefore urgently required to determine treatment eligibility, as the therapeutic window narrows with progressive neurological deterioration.

This case ultimately underscores the imperative of comprehensive neuroimaging, including MR spectroscopy, in any child presenting with neurological regression- even when a structural explanation appears adequate. The presence of a VP shunt and communicating hydrocephalus, while a legitimate cause of neurological dysfunction, should not preclude systematic evaluation for a concurrent metabolic or demyelinating disorder when the clinical or imaging profile is not fully accounted for by the structural abnormality alone. Schoenmakers et al. (2022) emphasised that knowledge of the early MRI signs of MLD- particularly corpus callosum involvement present in 94% of symptomatic early-juvenile patients- is essential for expediting diagnosis and enabling timely treatment [7]. The diagnostic delay reported across multiple international cohorts, with a median exceeding 230–257 days from first symptoms to confirmed diagnosis [9], carries real and irreversible neurological cost. In a disease where the timing of intervention is the single most important determinant of outcome, the radiologist and the clinician must maintain MLD on the differential in any child with unexplained white matter disease, irrespective of co-existing structural pathology.

4. Conclusion

Juvenile metachromatic leukodystrophy is a rare but diagnostically treacherous lysosomal storage disorder that may lurk undetected behind seemingly adequate structural explanations for neurological decline. This case demonstrates that the presence of communicating hydrocephalus and a functioning VP shunt does not exclude a concurrent, progressive demyelinating disease, and that milestone regression in such a setting demands a systematic multiparametric MRI evaluation rather than attribution to the known structural abnormality alone. The characteristic constellation of bilateral periventricular and deep white matter T2/FLAIR hyperintensities, significant corpus callosum thinning, patchy post-contrast enhancement indicating active demyelination, facilitated diffusion on DWI, and — most critically — the MR spectroscopic signature of elevated choline, lipid peaks, and markedly reduced NAA collectively pointed to juvenile MLD as the unifying diagnosis in our patient. This case reinforces that MR spectroscopy is not an optional adjunct but an indispensable tool in the evaluation of any child with unexplained white matter disease and neurological regression, as it provides metabolic evidence of the underlying pathological process that conventional sequences alone cannot furnish. Radiologists and clinicians must therefore maintain a high index of suspicion for leukodystrophic processes in children with neurological regression, regardless of co-existing structural pathology, and must not allow a prior diagnosis to foreclose the diagnostic horizon.

Ethical Statement

Written informed consent was obtained from the patient's parent/legal guardian for publication of this case report and accompanying images. Every effort has been made to protect the patient's identity, and no identifying information has been disclosed.

References

[1] Shaimardanova AA, Chulpanova DS, Solovyeva VV, Mullagulova AI, Kitaeva KV, Allegrucci C, et al. Metachromatic leukodystrophy: diagnosis, modeling, and treatment approaches. Front Med (Lausanne). 2020;7:576221.
[2] Polten A, Fluharty AL, Fluharty CB, Kappler J, von Figura K, Gieselmann V. Molecular basis of different forms of metachromatic leukodystrophy. N Engl J Med. 1991;324(1):18–22.
[3] Chang SC, Bergamasco A, Bonnin M, Arredondo Bisoño T, Moride Y. A systematic review on the birth prevalence of metachromatic leukodystrophy. Orphanet J Rare Dis. 2024;19(1):75.
[4] Feldmann J, Martin P, Bender B, Laugwitz L, Zizmare L, Trautwein C, et al. MR-spectroscopy in metachromatic leukodystrophy: a model free approach and clinical correlation. NeuroImage Clin. 2023;37:103291.
[5] Cheon JE, Kim IO, Hwang YS, Kim KJ, Wang KC, Cho BK, et al. Leukodystrophy in children: a pictorial review of MR imaging features. Radiographics. 2002;22(3):461–76.
[6] Eichler F, Grodd W, Grant E, Sessa M, Biffi A, Bley A, et al. Metachromatic leukodystrophy: a scoring system for brain MR imaging observations. AJNR Am J Neuroradiol. 2009;30(10):1893–7.
[7] Schoenmakers DH, Groeschel S, Caro-Llopis A, Faber J, Kehrer C, Krägeloh-Mann I, et al. Recognizing early MRI signs (or their absence) is crucial in diagnosing metachromatic leukodystrophy. Ann Clin Transl Neurol. 2022;9(12):1989–2001.
[8] Groeschel S, Kehrer C, Engel C, Dali CI, Bley A, Steinfeld R, et al. Metachromatic leukodystrophy: natural course of cerebral MRI changes in relation to clinical course. J Inherit Metab Dis. 2011;34(5):1095–102.
[9] Mohajer A, Sevagamoorthy A, Bean K, Mutua S, Pang F, Adang LA. Characterizing diagnostic delays in metachromatic leukodystrophy: a real-world data approach. J Inherit Metab Dis. 2025. doi:10.1002/jimd.70049.
[10] Kohlschütter A, Bley A, Brockmann K, Gärtner J, Krägeloh-Mann I, Õunap K, et al. Leukodystrophies and other genetic metabolic leukoencephalopathies in children and adults. Brain Dev. 2010;32(2):82–9.
[11] Desai J, Grimm J. Communicating hydrocephalus in metachromatic leukodystrophy. *Pediatr Neurol.* 2013;49(4):294–5. doi:10.1016/j.pediatrneurol.2013.02.006
[12] Kim TS, Kim IO, Kim WS, Choi YS, Lee KS, Kim WH, et al. MR of childhood metachromatic leukodystrophy. *AJNR Am J Neuroradiol.* 1997;18(4):733–8.
[13] Sener RN. Metachromatic leukodystrophy: diffusion MR imaging findings. *AJNR Am J Neuroradiol.* 2002;23(8):1424–6.
[14] Neyaz Z, Malik R, Nath K. Proton MR spectroscopy in leukodystrophies. *Egypt J Radiol Nucl Med.* 2015;46(4):939–48.

[15] Lewis E, Sondhi V, Aziz A, et al. Metachromatic leukodystrophy presenting with multiple cranial nerve and lumbosacral nerve root enhancement without white matter changes. *Children (Basel).* 2025;12(3):275. doi:10.3390/children12030275
[16] Groeschel S, Kühl JS, Bley AE, Kehrer C, Weschke B, Döring M, et al. Long-term outcome of allogeneic hematopoietic stem cell transplantation in patients with juvenile metachromatic leukodystrophy compared with nontransplanted control patients. *JAMA Neurol.* 2016;73(9):1133–40. doi:10.1001/jamaneurol.2016.2067
[17] Fumagalli F, Calbi V, Natali Sora MG, et al. Lentiviral haematopoietic stem-cell gene therapy for early-onset metachromatic leukodystrophy: long-term results from a non-randomised, open-label, phase 1/2 trial and expanded access. *Lancet.* 2022;399(10322):372–83. doi:10.1016/S0140-6736(21)02017-1